

Relativistic effects in the two-nucleon system

M. J. Zuilhof and J. A. Tjon

Institute for Theoretical Physics, Princetonplein 5, P.O. Box 80.006, 3508 TA Utrecht, The Netherlands

(Received 24 December 1980)

The Gross approximation to the Bethe-Salpeter equation is investigated using a one-boson-exchange model for the nucleon-nucleon interaction. In particular, it is shown that the inclusion of corrections from the two-pion direct-box diagram to the driving force in general does not yield phase shifts closer to those obtained from the Bethe-Salpeter equation. Moreover, the cross-box contributions lead in the quasipotential approach to a non-Hermitian interaction at all energies. The electromagnetic form factors of the deuteron are calculated for various sets of potential parameters which give reasonable scattering parameters. A detailed analysis is presented of the relativistic and mesonic exchange current corrections to the nonrelativistic limit. As a result it is shown that the usual treatment of mesonic exchange currents for both pseudovector and pseudoscalar pion-nucleon interaction is not correct since other non-negligible contributions should be taken into account.

NUCLEAR STRUCTURE NN system, quasipotential equations compared with Bethe-Salpeter equations. Effect of one-loop diagrams. Electromagnetic form factors. Comment on meson-exchange-current calculations.

I. INTRODUCTION

The problem of meson-exchange-current (MEC) effects on the electromagnetic properties of nuclei has attracted considerable attention in recent years. In particular, it was found that the so-called pair excitation current contributes a large correction to the charge form factor of the deuteron at moderate momentum transfers, if the estimates are made within the framework of perturbation theory. However, it is not clear whether this treatment is consistent since some aspects of the relativistic and dynamical effects are neglected in this approach. In a previous paper,¹ hereafter referred to as I, we reported on calculations of the electromagnetic form factors of the deuteron using a field theoretical one-boson-exchange (OBE) model, where all these aspects are treated in a correct way. We have shown that within such a model the resulting form factors are close to the ones obtained from a nonrelativistic calculation, suggesting that a consistent treatment would lead to smaller corrections than those found from the conventional perturbative calculations.

Since it is not clear how to compare the results from the Bethe-Salpeter equation (BSE) with those obtained from a nonrelativistic potential model in direct way, it is natural to investigate this problem in a quasipotential (QP) model which approximates the four-dimensional BSE by a relativistic three-dimensional equation. In this paper we study various aspects of one particular QP model, introduced by Gross.² In Sec. II we briefly introduce the QP equations. The driving force for these equations consists of the exchange of π , η ,

ϵ , ρ , δ , and ω mesons and is the same as in I. In Sec. III we discuss the convergence of the phase shift parameters in the Gross model to the BSE results by introducing correction terms in the driving force arising from the direct-box diagram. In general, we find that the inclusion of the pion direct box does not bring the results closer to those of the BSE.

Since all two-pion-exchange (TPE) contributions are expected to be important for the description of the nuclear force, we may consider the inclusion of the cross-box diagram in the Gross model. In Sec. IV we discuss the specific problems encountered. In particular, it is found that the Gross approximation leads to a spurious imaginary part of the potential which is present at all energies. In Sec. V the electromagnetic (em) form factors are calculated for the various potentials obtained in the study of the two-nucleon system. In general, they are close to the nonrelativistic results of the Reid soft-core interaction. Section VI is devoted to the study of the various corrections to the nonrelativistic limit. Both pseudoscalar (PS) and pseudovector (PV) theory for the pion-nucleon coupling are analyzed. We show that, for pseudoscalar coupling, there is a non-negligible contribution from the two-pion-exchange current. It is of the same order as the so-called pair-excitation-current contribution and of opposite sign. As a result the various contributions compensate each other leading to much smaller effects than originally suggested. These results are in accordance with those found previously³ for PV coupling. In the last section some concluding remarks are made.

II. THE GROSS APPROXIMATION

The general procedure used to approximate the BSE by a quasipotential equation (QPE) is well known.⁴ For convenience we shall recapitulate some essential formulas.

The BSE for the T matrix, in operator notation, reads

$$\phi = K - KS\phi, \quad (2.1)$$

where S is the two-nucleon propagator and K the driving term, which consists of the sum of all two-nucleon irreducible diagrams. The first step towards a QPE is to replace the BSE by a set of two coupled equations,

$$\phi = W - Wg\phi, \quad (2.2a)$$

$$W = K - K(S - g)W, \quad (2.2b)$$

which are completely equivalent to the BSE, assuming that all equations allow for solutions. The new propagator g is chosen in such a way that it reproduces the two-particle elastic unitarity condition at all energies $s \geq (2m)^2$, when W is Hermitian:

$$\phi - \phi^\dagger = \phi^\dagger (g^\dagger - g)\phi = 2\pi i \int \phi^\dagger \phi, \quad (2.3)$$

where the sum runs over all on-mass-shell intermediate states. Furthermore, g is required to reduce the four-dimensional integral in Eq. (2.2a) to a three-dimensional integral, resulting in an equation analogous to the Lippmann-Schwinger equation of potential theory.

These two requirements are certainly not enough to determine g uniquely. There still exist several families of solutions, as was first pointed out by Yeas.⁵ Two families have been used extensively, the Blankenbecker-Sugar (BbS)⁶ and the Gross² type of propagator. The main difference between the two is the way in which they treat the relative energy variable in the intermediate states, i.e., the reduction to a three-dimensional integral. The BbS propagator divides the energy equally over the two nucleons in the center of mass (c.m.) frame, i.e., puts them equally far off the mass shell, by setting the relative energy equal to zero in that frame. In the Gross approximation one of the nucleons is put on the mass shell in all intermediate states.

We may now assume that a reasonable approximation to the kernel W is obtained by taking only the lowest order term in Eq. (2.2b),

$$W \simeq K. \quad (2.4)$$

Using for K the same OBE model as in Ref. 1, the equations reduce after partial wave decomposition to a coupled set of integral equations in one

continuous variable. In most of the calculations, unless otherwise stated, we use the pseudovector coupling for the pion-nucleon interaction. The reduction is completely analogous to that of the BSE.⁷

Instead of the propagator of the BSE,

$$S(P, p) = \left(\frac{\not{P}^{(1)}}{2} + \not{p}^{(1)} - m \right)^{-1} \left(\frac{\not{P}^{(2)}}{2} - \not{p}^{(2)} - m \right)^{-1}, \quad (2.5)$$

we have the Gross propagator, given in the c.m. frame as

$$g(P, p) = \left(\frac{\not{P}^{(1)}}{2} + \not{p}^{(1)} + m \right) \left(\frac{\not{P}^{(2)}}{2} - \not{p}^{(2)} + m \right) \times (-2\pi i) \frac{\delta(p_0 - E + E_p)}{2E_p \left[\left(\frac{P}{2} + p \right)^2 - m^2 + i\epsilon \right]}, \quad (2.6)$$

with $E = \sqrt{s}/2$. The δ function restricts particle two to the mass shell, and selects only positive-energy spinors for this particle:

$$g(P, p) = 2\pi i \delta(p_0 - E + E_p) \times \left[\frac{\sum_{\lambda_1} U_{\lambda_1}(\vec{p}) \bar{U}_{\lambda_1}(\vec{p})}{2(E_p - E - i\epsilon)} - \frac{\sum_{\lambda_1} W_{\lambda_1}(\vec{p}) \bar{W}_{\lambda_1}(\vec{p})}{2E} \right] \times \left[\sum_{\lambda_2} U_{\lambda_2}(\vec{p}) \bar{U}_{\lambda_2}(\vec{p}) \right], \quad (2.7)$$

where the helicity spinors are defined in Appendix B of I. As a result the number of intermediate states is reduced from eight (for the BSE) to four. In the spectroscopic notation ${}^3L_J^{\rho_1}$, where ρ_1 is the energy-spin index for the off-mass-shell particle (conventionally taken as particle 1), the states for $J \neq 0$ are

$$\begin{aligned} & {}^3(J-1)_J^+, {}^3(J+1)_J^+, {}^1J_J^-, {}^3J_J^- \text{ (coupled triplet),} \\ & {}^3J_J^+, {}^1J_J^+, {}^3(J-1)_J^-, {}^3(J+1)_J^- \text{ (uncoupled triplet),} \\ & {}^1J_J^+, {}^3J_J^+, {}^3(J-1)_J^-, {}^3(J+1)_J^- \text{ (singlet),} \end{aligned} \quad (2.8)$$

and the states for $J=0$ are

$$\begin{aligned} & {}^3P_0^+, {}^1S_0^- \text{ (coupled triplet),} \\ & {}^1S_0^+, {}^3P_0^- \text{ (singlet).} \end{aligned} \quad (2.9)$$

In addition to the physical channels, there occur channels which either contain a negative-energy state or are odd in the relative energy, which means that they vanish on the mass shell. In the following we will also consider the situation that we keep only the physical channels in the intermediate states. This will be called the two-

channel approximation, although there is, of course, only one channel in the uncoupled waves. This truncation has no effect on the two particle unitarity.

The solution of the one-dimensional integral

equations is found by employing the Noyes-Kowalski technique.⁸ The resulting equations are solved by discretization and matrix inversion. As a check, the solution is also calculated by constructing the Padé approximants to the multiple scatter-

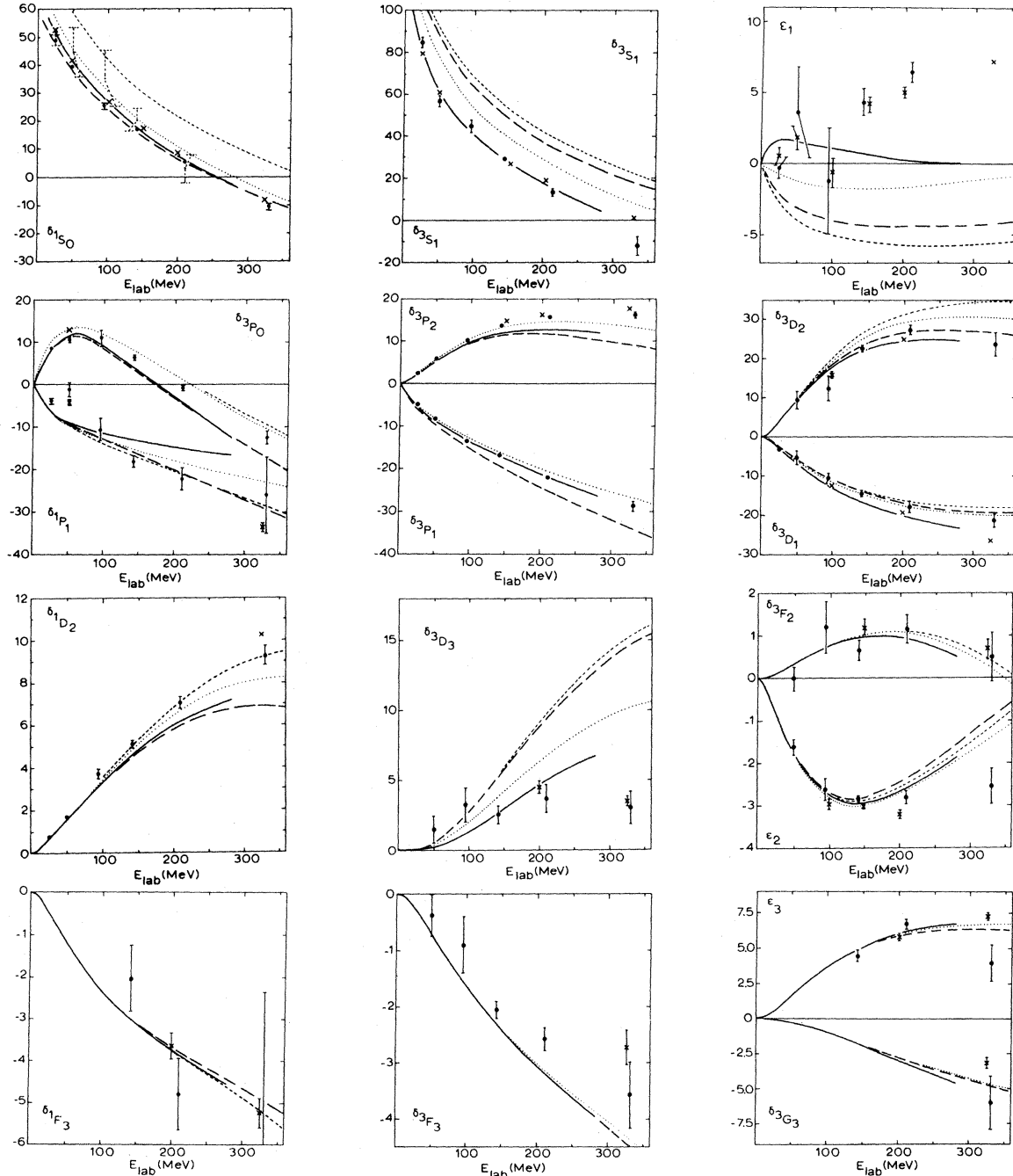


FIG. 1. The phase shifts for the BbS (···) and the Gross equation (---) compared with those of the BSE (—) with the same driving force. For Gross we show the results for the 4 ch equation and of the 2 ch equation (- - -). In the 3P_2 , 3P_1 , and 3F_3 channel the 2 ch Gross results are identical to the BbS results. The 4 ch results coincide with those of BbS in the 3F_2 and 1F_3 channel, and with the 2 ch Gross equation for ϵ_3 . For the 3G_3 wave the 2 ch Gross is between the BbS and the 4 ch Gross. The data points are the energy-independent fits of Ref. 9, (●), and of Ref. 10, (⊗).

ing series. Both solutions are compatible to three or four decimals. The results are stable with respect to the number and the distribution of mesh-points when typically 14 integration points are used.

To get some insight into the effects of the QP approximation, the phase shifts from the Gross equation have been calculated with the same coupling parameters as used in the BSE. The results are plotted in Fig. 1, where, in addition, the effect of the negative-energy states is demonstrated. For comparison we have also drawn the results for the BbS equation with only positive-energy states. The effects in the higher partial waves, such as the F and G waves, are small. This reflects the fact that they are essentially given by the Born approximation. The most drastic changes are found in the 1S_0 , 3S_1 , and 3D_3 channels. The latter is somewhat disturbing since it is a D wave. It should be noted, however that the Born approximation to the 3D_3 channel is rather bad and that the two- and higher-boson exchanges are very important. The strong deviation indicates that the QP approximation does not do a very good job in simulating these higher order diagrams. The large changes in the S waves are less worrisome because in these channels short range effects are important. The same holds for the ϵ_1 because this parameter is extremely sensitive to the details of the interaction.

The Gross equation with the negative-energy states included gives for the D waves a better approximation to the BSE than without. In general, these states are not negligible, especially at higher energies, and they give rise to an overall repulsion with the exception of the 1F_3 wave. On the

other hand, solving the BSE in the approximation that all the negative-energy states are dropped yields results which are close to those of the complete BSE calculation with exception of the 3P_0 wave. Some results are given in Table I. These results indicate that especially in the uncoupled P and D waves a strong cancellation should take place in the Gross equation between the contributions from negative-energy states and the off-mass-shell p_0 dependence in order to recover the BSE results from the QP model.

The two-channel Gross equation gives a reasonable fit to the data with the parameters used in Ref. 3, to fit the 3S_1 - 3D_1 channel, when $g_\epsilon^2/4\pi$ is set to 6.55 to get the bound state energy at -2.225 MeV. The fit is shown in Fig. 2, while the numerical values of the parameters are summarized in Table II.

Inclusion of the negative-energy states increases the splitting between the 1S_0 and 3S_1 phase shifts, and gives a strong repulsion in the P and D waves. We have varied the g_ω , g_ϵ , g_ρ^T/g_ρ^V , and Λ to obtain a new qualitative fit. The procedure thereby was that g_ρ^T/g_ρ^V was set to obtain the correct splitting between the 1S_0 and 3S_1 phase shifts. The g_ϵ was fixed by the binding energy so that only the g_ω and the cutoff mass were free to vary. The other parameters are of less importance since they do not change the phase shifts strongly. The new parameters for the four-channel fit are given in Table II. The very bad shape of the 3D_1 and the ϵ_2 is the price paid for obtaining a good fit for the P waves and the 1D_2 and 3D_2 waves, and is associated with the low value for Λ and the rather high g_ρ^T/g_ρ^V . The strong attraction in the 3D_3 is insensitive to all the variations of the parameters so that we are led to conclude that it is a deficiency of the approximation. Figure 1 shows that the BbS approximation has the same problem but not as strong.

The fact that the negative-energy states have a relatively small influence is due to the use of PV coupling for the pion. The more commonly used PS coupling gives similar results when we restrict ourselves to positive-energy states only. The coupling to the negative-energy states is so strong, however, that it seems to be impossible to refit the phase shifts within reasonable variations of the parameters. For example, to obtain a bound state at the deuteron energy $g_\epsilon^2/4\pi$ has to be increase to about 25 while $g_\omega^2/4\pi$ is lowered to 5. The 3S_1 - 3D_1 channel is then relatively well described, although the S -wave phase shifts are about 8° too low, but the other channels remain in poor condition. A similar behavior is found in the the BSE, so that this is not a particular feature of the QP approximation.

TABLE I. Comparison of the phase shifts obtained from Bethe-Salpeter equation with (8 ch) and without (2 ch) negative-energy states at two different energies.

| | 150 MeV | | 250 MeV | |
|--------------|---------|--------|---------|--------|
| | 2 ch | 8 ch | 2 ch | 8 ch |
| 1S_0 | 14.03 | 16.23 | -1.12 | 0.91 |
| 3S_1 | 27.62 | 27.31 | 9.66 | 9.14 |
| 3D_1 | -17.06 | -17.07 | -22.15 | -22.21 |
| ϵ_1 | 0.60 | 0.59 | 0.15 | 0.034 |
| 3P_0 | 6.20 | 2.83 | -3.87 | -9.11 |
| 1P_1 | -13.23 | -13.37 | -15.34 | -16.17 |
| 3P_1 | -17.37 | -17.83 | -23.71 | -24.66 |
| 3P_2 | 12.69 | 11.96 | 13.76 | 12.46 |
| 3F_2 | 0.96 | 0.96 | 0.75 | 0.73 |
| ϵ_2 | -2.95 | -2.93 | -2.24 | -2.24 |
| 1D_2 | 4.91 | 4.82 | 7.06 | 6.79 |
| 3D_2 | 23.35 | 22.34 | 26.87 | 24.72 |
| 3D_3 | 3.02 | 3.00 | 6.06 | 6.00 |

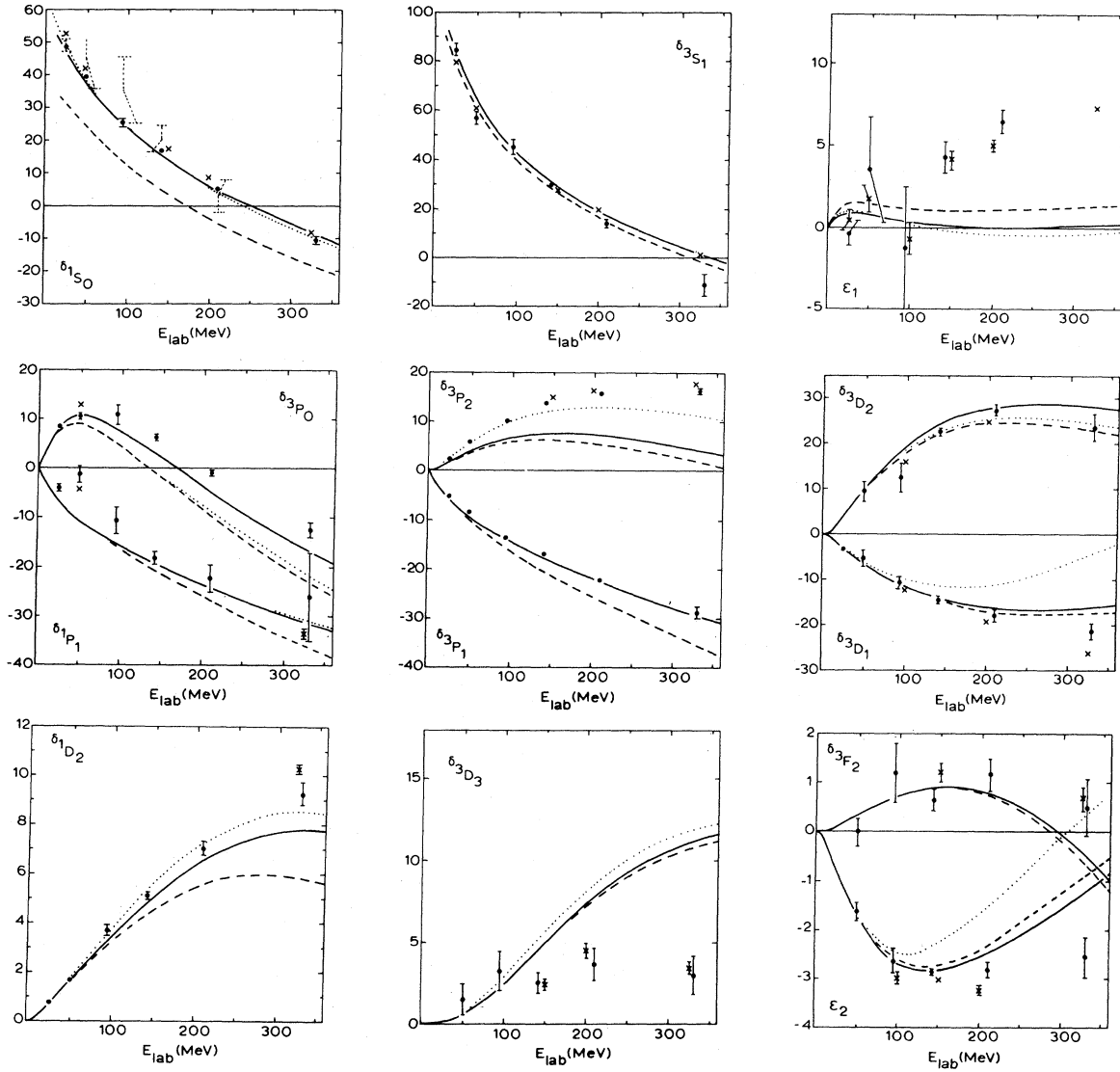


FIG. 2. The phase shifts for the 2 ch fit (—), and the effect of including the negative-energy states (- - -). The dotted curves are the result for the 4 ch fit. For the 3S_1 the 4 ch result lies between the other two curves. In the 1P_1 and 3P_1 waves the refitted 4 ch equation gives results identical to the 2 ch equation, while for the 3F_2 wave the refitting had no effect. The experimental data are the same as in Fig. 1.

TABLE II. The coupling parameters for the Bethe-Salpeter equation, the Gross equation with only positive-energy states, and for the Gross equation with all states.

| | $\frac{g_\pi^2}{4\pi}$ | $\frac{g_\epsilon^2}{4\pi}$ | $\frac{g_\omega^2}{4\pi}$ | $\frac{g_\rho^2}{4\pi}$ | $\frac{g_\rho^T}{g_\rho^V}$ | $\frac{g_\delta^2}{4\pi}$ | $\frac{g_\eta^2}{4\pi}$ | Λ^2 (nucleon mass ²) |
|--------------------------------------|------------------------|-----------------------------|---------------------------|-------------------------|-----------------------------|---------------------------|-------------------------|---|
| BS | 14.2 | 7.3 | 11.0 | 0.43 | 6.0 | 0.33 | 3.09 | 1.9 |
| Gross (positive energy only) | 14.2 | 6.55 | 12.0 | 0.43 | 6.8 | 0.33 | 3.09 | 1.5 |
| Gross (including negative energy) | 14.2 | 7.02 | 10.0 | 0.43 | 7.6 | 0.33 | 3.09 | 1.2 |

III. THE DIRECT BOX

In the previous section we studied the Gross equation in the scattering region assuming that the kernel of the equation may be approximated by Eq. (2.4). As is seen the results can be quite different from those obtained from the BSE. One may hope that the situation is improved by the introduction of the next order correction to W in Eq. (2.2b), resulting in a better representation of the BSE. The quality of such an approximation has, to our knowledge, only been investigated for the case of scalar nucleons interacting via scalar mesons.¹¹

$$B(q, p; E) = -\frac{i}{4\pi^3} \left(\frac{g^2}{4\pi}\right)^2 (\vec{\tau}^{(1)} \cdot \vec{\tau}^{(2)})^2 \int d^4k_1 F(k_2) \frac{\gamma_5^{(1)} \not{k}_2^{(1)} \left(\frac{P}{2} + \not{k} + m\right)^{(1)} \not{k}_1^{(1)} \gamma_5^{(1)}}{\left[\left(\frac{P}{2} + k\right)^2 - m^2 + i\epsilon\right]} \frac{\gamma_5^{(2)} \not{k}_2^{(2)} \left(\frac{P}{2} - \not{k} + m\right)^{(2)} \not{k}_1^{(2)} \gamma_5^{(2)}}{\left[\left(\frac{P}{2} - k\right)^2 - m^2 + i\epsilon\right]} F(k_1), \quad (3.2)$$

where $F(k)$ is a shorthand notation for the pion propagator with the cutoff factor

$$F(k) = \frac{\Lambda^2}{(k^2 - \mu^2 + i\epsilon)(k^2 - \Lambda^2 + i\epsilon)^2}. \quad (3.3)$$

The momenta k , k_1 , and k_2 are defined in Fig. 3. The expression (3.2) is reduced to a set of integrals of the form

$$\begin{aligned} D0 &= -\frac{i}{4\pi^3} \int d^4k_1 \Delta, \\ D1_\mu &= -\frac{i}{4\pi^3} \int d^4k_1 k_{1\mu} \Delta, \\ D2_{\mu\nu} &= -\frac{i}{4\pi^3} \int d^4k_1 k_{1\mu} k_{1\nu} \Delta, \end{aligned} \quad (3.4)$$

where Δ contains the denominators of (3.2); i.e., $D0$ is essentially the direct box for scalar particles. We also need the same type of integrals where some of the factors in the denominator have been canceled against scalar products of the momenta, which are encountered in working out the nominator of (3.2). The integrals (3.4) can be expressed in terms of scalar form factors and tensors formed from the external momenta P , q , and

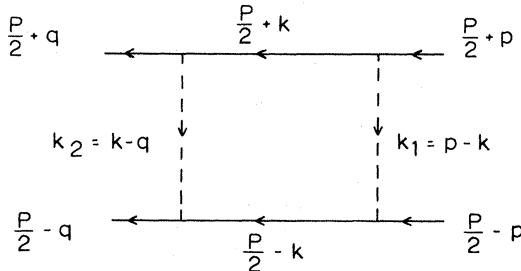


FIG. 3. Definition of the momenta used in the direct box.

In this section we examine this approximation for the more realistic case with spin by replacing the kernel in the Gross section by

$$W \simeq K - K(S - g)K. \quad (3.1)$$

Moreover, we will confine ourselves to contributions to the second term from pion and omega exchange. In order to calculate W we need to evaluate the direct-box diagram, shown in Fig. 3, for the general case of particles with spin.

A detailed account of the calculation will be reported elsewhere. Here we give only the essential steps for the two-pion box diagram:

p , as described in Ref. 12. These scalar form factors can be calculated with the program FORMF written by Veltman.¹³

The partial wave projection of the resulting expression is, in principle, similar to that of the one-boson-exchange kernel, but algebraically more complicated. It is carried out with the help of the algebraic program SCHOONSCHIP.¹⁴ The angular integration cannot be performed analytically since the form factors are angle dependent. In practice it is very advantageous to calculate all partial waves in one run, because the angular integration takes only about one percent of the time needed to evaluate the scalar form factors, which are (of course) the same for all partial waves. We calculated all partial waves up to and including $J=3$, which makes eleven partial waves. It takes approximately 11 min on a Cyber 175 to calculate the potential matrix elements of one box diagram for a set of 14 off-shell momenta at a given c.m. energy.

The code has been tested by comparing the results with the box diagram calculated by iterating the BSE, which is slower and less accurate. Within the numerical accuracy the same results were found. We also checked the imaginary part which can be evaluated by hand and also by FORMF.

In Fig. 4 we show the phase shifts calculated from the Gross equation with the kernel (3.1), where we took only the pion contribution to the term $K(S - g)K$. Again, all parameters are the same as those for the BSE fit used in I. For reference we also plotted the BSE and Gross OBE result. For S , P , and D waves we find no convergence to the BSE phase shifts. In general, the effect of the pion box is very strong. Depending on the partial wave channel, the difference between

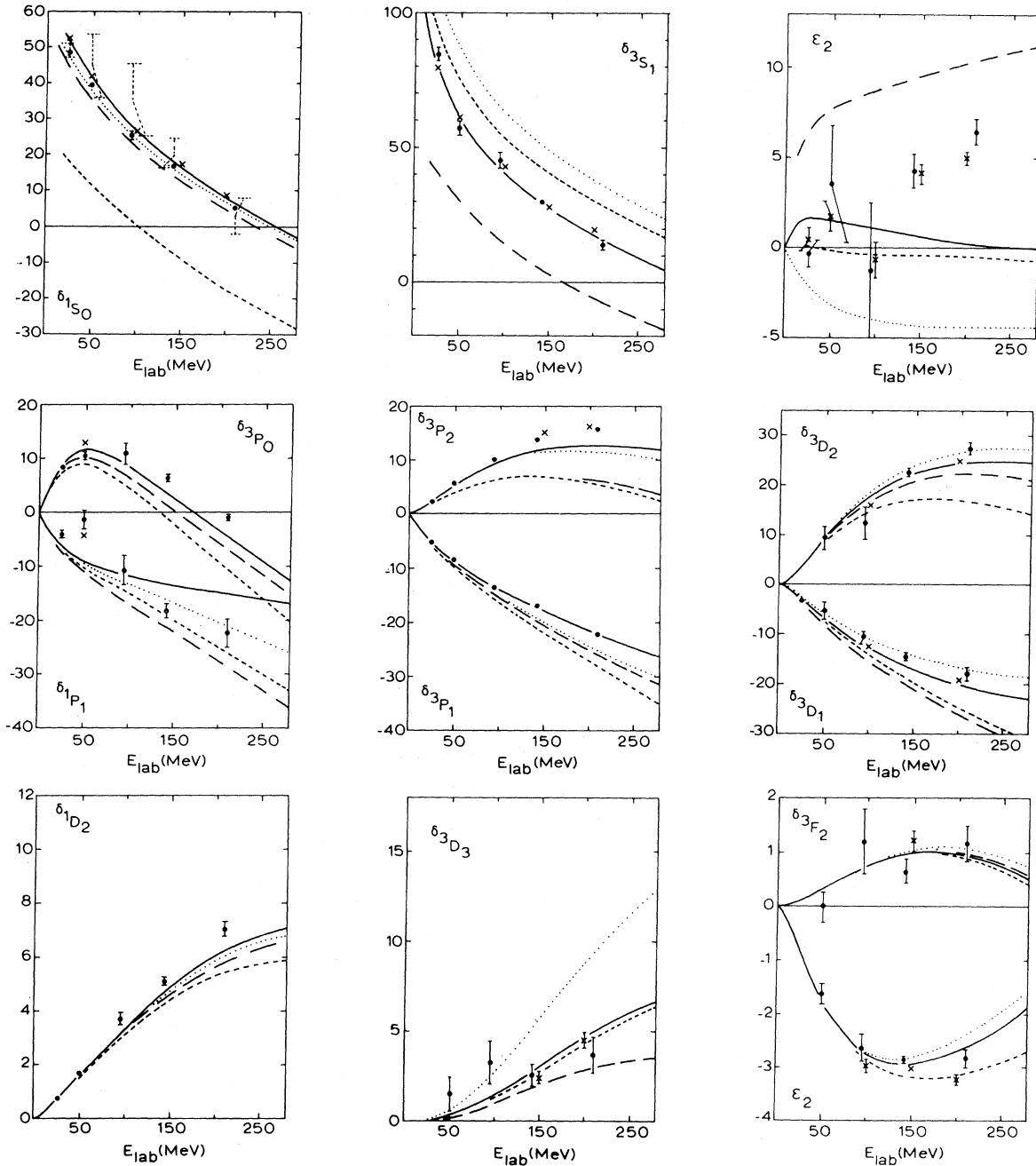


FIG. 4. The phase shifts for the BSE (—) compared to those for the Gross equation (···) as in Fig. 1, and the effects of the pion box (---) and of the pion plus omega boxes (- - -). The 3P_0 phase shift for Gross coincides with the BSE on this scale. For the ϵ_2 the Gross equation with the pion box included gives the same result as the BSE.

the QPE and the BSE is either overcompensated or becomes larger. This should be contrasted with the results obtained in the case of scalar nucleons interacting in S waves.¹¹ Also note the strong influence on the 3D_3 . Furthermore, the difference between the Gross direct box and the two-pion box is repulsive for all partial waves shown in Fig. 4. We have also calculated the effect of the ω meson;

i.e., we now have four correction terms in (3.1):

$$(K_{\pi} + K_{\omega})(S - g)(K_{\pi} + K_{\omega}). \quad (3.5)$$

This does not improve the situation, as can be seen from Fig. 4. There is a very strong effect in the S waves, but even in the D waves the changes are appreciable. We clearly need more attraction in the P and D waves. We must conclude that cor-

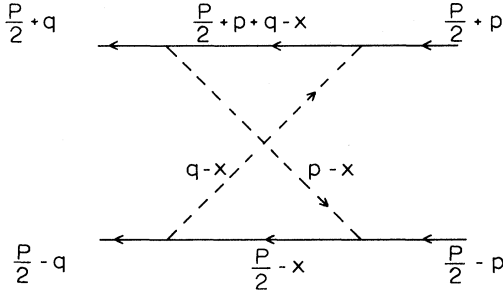


FIG. 5. The crossed box.

recting the kernel of the QPE for the direct box of pions does not yield results that are closer to those of the BSE. A possible improvement might be found in the inclusion of other mesons like ρ and ϵ into the direct box graph. However, since the effects are generally so strong, we should also expect that the corrections from the multiple-loop diagrams are also important. The calculation of both types of corrections will be very time consuming and as a result the QP approach would not be advantageous anymore as compared to the use of the original BSE.

IV. THE CROSSED BOX

Analogous to the direct box we may evaluate the crossed-box contribution to the quasipotential W . However, due to the specific choice of the relative energy variable in the external momenta, we encounter spurious singularities which destroy two-particle unitarity at all energies.

In general, there exist two kinds of singularities in box diagrams for real off-mass-shell momenta. The first kind is the unitarity type of singularity. For the direct box they give rise to the cut for $\sqrt{s} > 2m$ and for $\sqrt{t} > 2\mu$. For the crossed box the singularities lie in the crossed channel $\sqrt{u} > 2m$ and also in the t channel $\sqrt{t} > 2\mu$. The second kind is of the instability type, i.e., the mass of one of the incoming or outgoing particles is larger than $(m + \mu)$. The singularities arise because the poles of certain propagators pinch the integration contour of the loop momentum.

For the BbS choice of the relative momenta, we find

$$u \leq 0 \text{ and } t \leq 0 \quad (4.1)$$

for all values of the external momenta, which is most easily seen in the c.m. frame. This assures that there are no unitarity type singularities in the boxes. The "masses" of the external particles are given by

$$\left(\frac{P}{2} + p\right)^2 = \left(\frac{P}{2} - p\right)^2 = \frac{s}{4} - \vec{p}^2$$

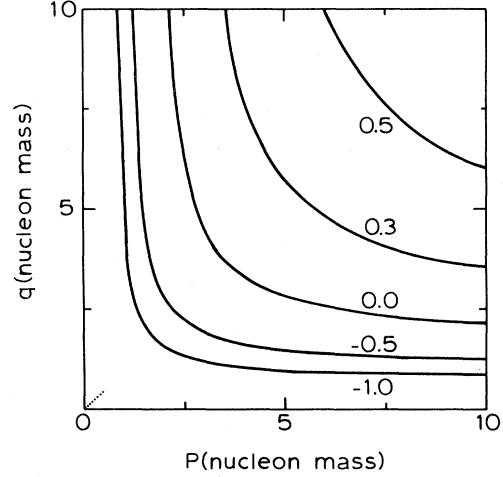


FIG. 6. The boundaries of the area where $\text{Im}X \neq 0$ in the p - q plane for different angles $z = \cos \theta$ between p and q . $\sqrt{s} = 2$. The dotted line represents the range of on-mass shell values as E_{1ab} runs from 0 to 350 MeV. $\text{Im}X$ is different from zero above the curves.

and (4.2)

$$\left(\frac{P}{2} + q\right)^2 = \left(\frac{P}{2} - q\right)^2 = \frac{s}{4} - \vec{q}^2$$

in the c.m. frame. This means that for $\sqrt{s} \leq 2(m + \mu)$, i.e., $E_{1ab} \leq 580$ MeV, there are no instability type singularities.

For the Gross choice we have

$$t = (p - q)^2 \leq 0$$

and (4.3)

$$u = (p + q)^2 = (E_q + E_p - \sqrt{s})^2 - (\vec{p} + \vec{q})^2,$$

where u can become arbitrarily large, independent of the energy (take, for example, $\vec{p} = -\vec{q}$). Furthermore, we find that the instability type of singularity occurs for $\sqrt{s} > 2m + \mu$, i.e., $E_{1ab} \geq 280$ MeV:

$$\left(\frac{P}{2} + p\right)^2 \leq (\sqrt{s} - m)^2 \text{ and } \left(\frac{P}{2} - q\right)^2 \leq (\sqrt{s} - m)^2. \quad (4.4)$$

The existence of the u -channel singularity is serious because it destroys two-particle unitarity at all energies when we approximate the quasipotential to fourth order in the coupling constant. In fact, one needs an infinite set of terms to restore unitarity in the elastic scattering region, $2m < \sqrt{s} < 2m + \mu$; apart from this the singularity presents numerical complications.

The condition $\sqrt{u} \geq 2m$ is satisfied when

$$E_p + E_q - \sqrt{s} \geq [(2m)^2 + (\vec{p} + \vec{q})^2]^{1/2}, \quad (4.5)$$

which is the condition that the poles of the two nucleon propagators can pinch the x_0 -integration contour. Taking the variables as defined in Fig. 5, in

the c.m. frame, the poles are at

$$\begin{aligned} x_0^{(1)} &= \frac{3\sqrt{s}}{2} - E_p - E_q + E_{\vec{p}+\vec{q}-\vec{x}} - i\epsilon, \\ x_0^{(2)} &= \frac{\sqrt{s}}{2} - E_x + i\epsilon, \end{aligned} \quad (4.6)$$

where the superscripts label the particles. The condition (4.5) defines a region in the (p, q) plane for a fixed angle between \vec{p} and \vec{q} and a given energy. This is sketched in Fig. 6.

Apart from constant factors, the crossed box for scalar particles (spin is irrelevant for this singularity) is given by

$$X = -i \int d^4x \left\{ [(p-x)^2 - \mu^2 + i\epsilon][(q-x)^2 - \mu^2 + i\epsilon] \left[\left(\frac{P}{2} - x \right)^2 - m^2 + i\epsilon \right] \left[\left(\frac{P}{2} + p + q - x \right)^2 - m^2 + i\epsilon \right] \right\}^{-1}. \quad (4.7)$$

For the imaginary part we find

$$\text{Im}X = \frac{\pi^2}{2} \int d^3x \frac{1}{E_x E_{\vec{p}+\vec{q}-\vec{x}}} [(E_x - E_p)^2 - \omega_{\vec{p}-\vec{x}}^2 + i\epsilon]^{-1} [(E_x - E_q)^2 - \omega_{\vec{q}-\vec{x}}^2 + i\epsilon]^{-1} \delta(\sqrt{s} - E_p - E_q + E_x + E_{\vec{p}+\vec{q}-\vec{x}}), \quad (4.8)$$

where $\omega_{\vec{p}} = (\vec{p}^2 + \mu^2)^{1/2}$.

The fact that the imaginary part is symmetric in \vec{p} and \vec{q} makes the crossed box contribution to W non-Hermitian and thus destroys unitarity. Evaluating, in the usual way, the imaginary part of the T matrix for a non-Hermitian potential we find

$$\phi^\dagger - \phi = \phi^\dagger (g^\dagger - g) \phi - 2i \phi^\dagger g^\dagger (\text{Im}W) g \phi, \quad (4.9)$$

where we used the fact that $\text{Im}W$ vanishes when one of the external relative momenta is on shell. This can be seen from (4.8). Take, for example, $E_p = \sqrt{s}/2$, then the argument of the δ function becomes

$$\frac{\sqrt{s}}{2} - E_q + E_x + E_{\vec{p}+\vec{q}-\vec{x}} \geq \frac{\sqrt{s}}{2} - E_q + [(2m)^2 + (p-q)^2]^{1/2} \geq \frac{\sqrt{s}}{2} - p = \frac{\sqrt{s}}{2} - \left(\frac{s}{4} - m^2 \right)^{1/2} > 0 \quad (4.10)$$

so that $\text{Im}X = 0$.

On the other hand, we expect that the contribution of $\text{Im}X$ to (4.9) will be small because it exists only for relatively large values of the momenta p and q . In principle, one could ignore this imaginary part and calculate the contribution of the real part of X to W . But then there is the numerical complication that the real part of X has a kink as shown in Fig. 7, for the value of $\cos\theta_{pq}$, where the imaginary part becomes different from zero:

$$-1 \leq \cos\theta_{pq} \leq \frac{\frac{s}{2} - \sqrt{s}(E_p + E_q) + E_p E_q - m^2}{pq}. \quad (4.11)$$

This forces us to split up the θ_{pq} integration as a function of p, q , and \sqrt{s} . In view of the above considerations we decided to examine the crossed box contribution only in the BbS approximation which will be discussed in a forthcoming paper.

V. THE DEUTERON FORM FACTORS

Having determined two sets of potential parameters which give a reasonable fit to the phase shifts at least in the S waves, we can now calculate the em properties of the deuteron. As usual we start from the expression for the matrix elements of the deuteron current in the Breit frame. We use the transformation properties of the vertex functions and the propagator to shift the boost op-

erators to the em vertex, as explained in I. It can be shown that the vertex functions satisfying the Gross equation have the same transformation properties under Lorentz transformations as the BS vertex functions:

$$\psi^M(p, P) = \Lambda^{(1)}(\mathcal{L}) \Lambda^{(2)}(\mathcal{L}) \psi^M(\mathcal{L}^{-1}p, \mathcal{L}^{-1}P). \quad (5.1)$$

Here p and P are, respectively, the relative and the total momentum of the two-particle system and Λ is the spinor representation of \mathcal{L} . The relativistic impulse approximation to the deuteron current can now be written in a form in which only the c.m. vertex functions appear, just as in I:

$$\begin{aligned} \langle P+q, M' | J_b^\mu | P, M \rangle \\ = \int d^3k \psi_{\text{c.m.}}^{M'\dagger}(\vec{k}') S\left(\frac{P_{\text{c.m.}}}{2} + k'\right) \\ \times \tilde{\Gamma}^\mu(q) S\left(\frac{P_{\text{c.m.}}}{2} + k\right) \Lambda_+(-\vec{k}) \psi_{\text{c.m.}}^M(\vec{k}). \end{aligned} \quad (5.2)$$

The em vertex contains the boost operators

$$\begin{aligned} \tilde{\Gamma}_\mu(q) &= \Lambda^{-1}(\mathcal{L}') \Gamma_\mu^{(1)}(q) \Lambda(\mathcal{L}) \\ &= [\Lambda(\mathcal{L}) \Gamma_\mu(q) \Lambda(\mathcal{L})]^{(1)} [\Lambda^2(\mathcal{L})]^{(2)}, \end{aligned} \quad (5.3)$$

where we used the fact that $\mathcal{L}' = \mathcal{L}^{-1}$ in the Breit frame. For Γ_μ we used the on-mass-shell form

$$\Gamma_\mu(q) = \gamma_\mu F_1(q^2) - \frac{1}{2M_N} \sigma_{\mu\nu} q^\nu F_2(q^2). \quad (5.4)$$

The propagator in the Gross approximation reads

$$S\left(\frac{P_{c.m.}}{2} + k\right) = \frac{\Lambda_+^{(1)}(\vec{k})}{2(E_p - E - i\epsilon)} - \frac{\Lambda_-^{(1)}(\vec{k})}{2E}, \quad (5.5)$$

where $E = M_D/2$. The positive- and negative-energy projection operators $\Lambda_{\pm}(\vec{k})$ are defined in the Appendix. In Eq. (5.2) we absorbed all normalization factors into the vertex functions. Owing to symmetry one only has to consider the diagram with the photon coupled to particle one. The relative momenta \vec{k}' and \vec{k} in (5.2) are related by the boost transformation

$$k' = \mathcal{L}\left(\mathcal{L}k + \frac{q}{2}\right), \quad (5.6)$$

where the zeroth component of k and k' is deter-

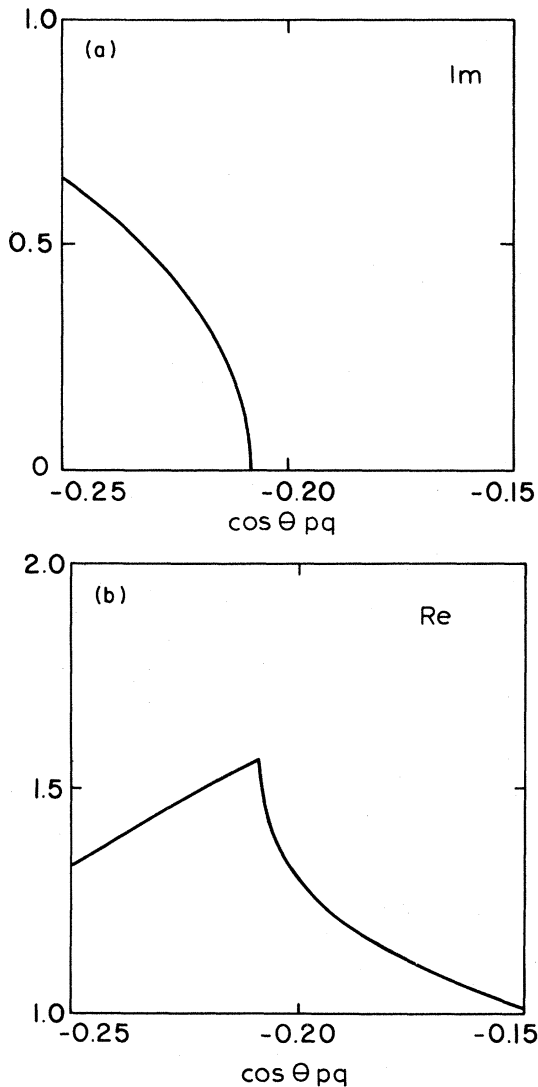


FIG. 7. (a) shows the threshold behavior of $\text{Im}X$ for $p=q=3$ and $E_{1ab}=100$ MeV, for the scalar crossed box. (b) shows the behavior of the corresponding real part.

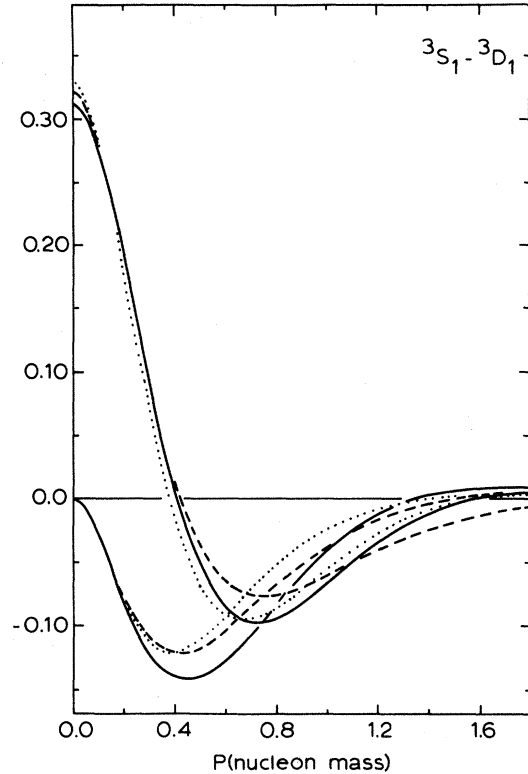


FIG. 8. The 3S_1 and 3D_1 components of the wave functions discussed in the text. The dashed line is the 4 ch Gross wave function of the PV model. The solid line is the Reid wave function. The wave function for the PS model discussed in Sec. VI is given by the dotted line.

mined by the Gross prescription

$$k_0 = E - E_k \quad \text{and} \quad k'_0 = E - E_{k'}. \quad (5.7)$$

For more details we refer to I.

We have calculated the vertex function for the two-channel and the four-channel fit described in Sec. II. The positive-energy components can be compared with the Reid wave functions in Fig. 8. The smaller D -wave component is characteristic for OBE models, which in general have a D -state probability varying from 4–5%, while for the Reid model $P_D = 6.4\%$. The negative-energy components are shown in Fig. 9. The static properties for the two models are given in Table III. We find that the results of the two-channel model are better as compared to experiment than those of the four-channel model. This is mainly due to the bad fit of the 3D_1 phase shift. In models which are fitted to the 3S_1 - 3D_1 channel and the higher partial waves, but not to the 1S_0 , we find, in general, static properties which are closer to the experimental values than those of this particular model. The electromagnetic form factors, Fig. 10, show

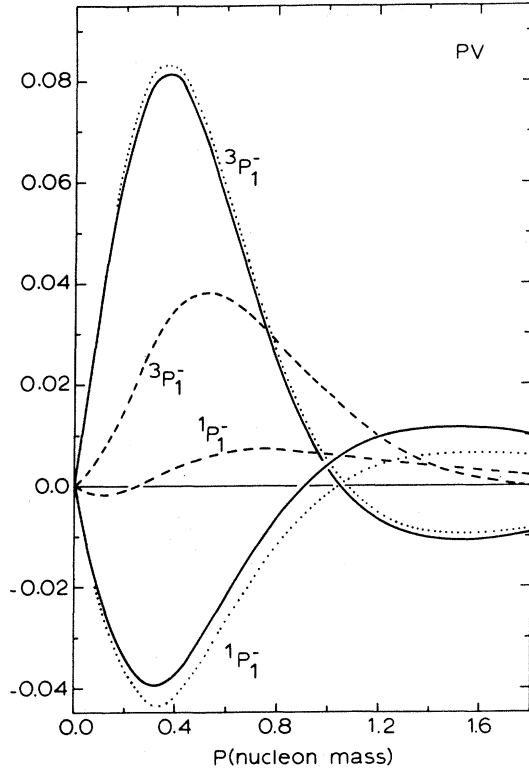


FIG. 9. The ${}^3P_1^-$ components of the wave function, calculated from the 4 ch PV model (—) and in the OPE approximation (---). The dotted line is the result when we take the OBE instead of the OPE.

qualitatively the same behavior as the Bethe-Salpeter form factors calculated in I.

VI. CORRECTIONS TO THE NONRELATIVISTIC LIMIT

In I we have shown that the em form factors as calculated for a Bethe-Salpeter model of the deuteron are very similar to those obtained from a nonrelativistic theory. The same result is found in the previous section for the Gross equation. These results are clearly in contradistinction to those of perturbative calculations carried out by several authors,^{15,16} but essentially in agreement with calculations for model wave functions.¹⁷ In

this section we analyze the various corrections to a nonrelativistic potential calculation within the QP approach using perturbation theory. We shall try to set up a more comprehensive and consistent calculation of the MEC and relativistic effects. In this analysis we shall allow for the possibility that the pion-nucleon interaction is given by either a PV or a PS coupling theory. For PS coupling we shall give arguments that the usual lowest order perturbative treatment of the negative-energy components is not sufficient, but that there are "higher order" corrections which are larger than the first order contributions.

The corrections to the nonrelativistic limit can be divided into the contributions arising from the negative-energy states in the deuteron wave function and the difference between the positive-state contribution and its nonrelativistic limit. We first consider the terms in the current matrix element that contain negative-energy states. To do so we write the deuteron current, Eq. (5.2), as in Eq. (A10) of the Appendix:

$$\langle P+q, M' | J_D^\mu | P, M \rangle = \int d^3k \sum_{\alpha, \beta} \phi_\alpha^{M'\dagger}(\vec{k}') S_\alpha(\vec{k}') \bar{\Gamma}_{\alpha\beta}^\mu S_\beta(k) \phi_\beta^M(\vec{k}), \quad (6.1)$$

where the sum runs over positive- and negative-energy states. The negative-energy-state contribution to the current is thus given by

$$\begin{aligned} \Delta \langle J_D^\mu \rangle_{\text{neg}} = & \int d^3k [\phi_+^{M'\dagger}(\vec{k}') S_+(\vec{k}') \bar{\Gamma}_{+-}^\mu S_-(k) \phi_-^M(\vec{k}) \\ & + \phi_-^{M'\dagger}(\vec{k}') S_-(\vec{k}') \bar{\Gamma}_{-+}^\mu S_+(k) \phi_+^M(\vec{k}) \\ & + \phi_-^{M'\dagger}(\vec{k}') S_-(\vec{k}') \bar{\Gamma}_{--}^\mu S_-(k) \phi_-^M(\vec{k})]. \end{aligned} \quad (6.2)$$

Since we consider this as a perturbation on the positive-energy part we expand all expressions to the lowest order in k/m and q/m . In the following we restrict ourselves to the charge operator $\mu = 0$. To lowest order we find

TABLE III. The static properties of the deuteron for the various models discussed in the text.

| | Q (mb) | $\mu_D \left(\frac{e}{2M_N} \right)$ | $\rho_{D/S}$ | P_D | P_{1P_1} | P_{3P_1} |
|------------|----------|---------------------------------------|--------------|-------|------------|------------|
| Gross 4 ch | 2.67 | 0.8726 | 0.0243 | 3.95 | 0.017 | 0.025 |
| Gross 2 ch | 2.71 | 0.8525 | 0.0250 | 4.74 | | |
| exp | 2.86 | 0.857406 | 0.0263(13) | | | |

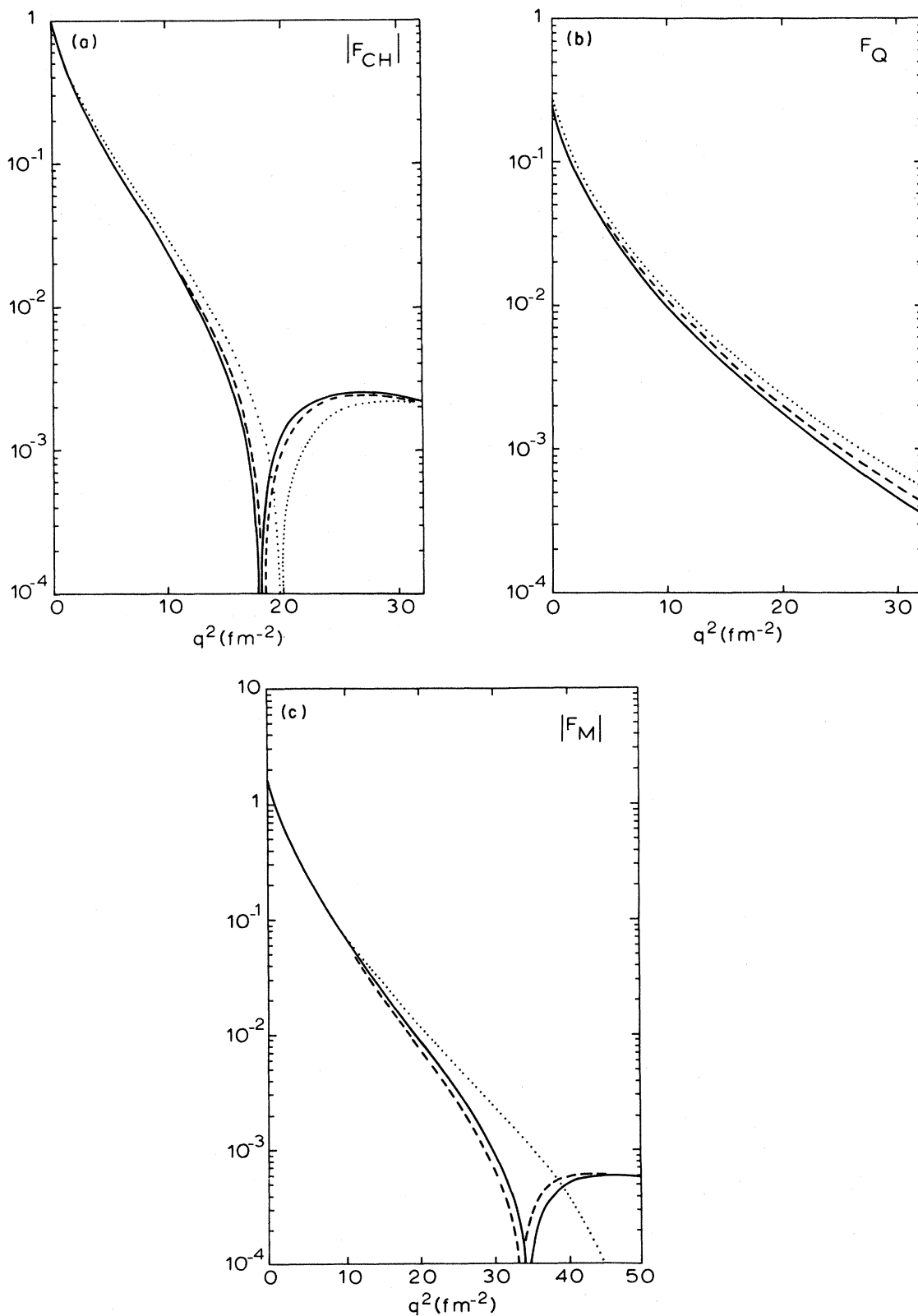


FIG. 10. The charge, quadrupole, and magnetic form factors of the deuteron for the 4 ch PV model (—) and the truncated model (---). For reference we also show the results for the Reid wave function (···).

$$\begin{aligned}
\vec{k}' &\simeq \vec{k} + \frac{\vec{q}}{2}, \\
S_+(k) &\simeq \frac{1}{\frac{k^2}{M_N} + E_B}, \\
\tilde{\Gamma}_{+-}^0 &\simeq -\tilde{\Gamma}_{-+}^0 \simeq \frac{\vec{q} \cdot \vec{\sigma}^{(1)}}{2M_N} \left(\frac{F_1^S}{2} + F_2^S \right) \mathbf{1}^{(2)}, \\
\tilde{\Gamma}_{--}^0 &\simeq -\mathbf{1}^{(1)} \mathbf{1}^{(2)} F_1^S.
\end{aligned} \tag{6.3}$$

To obtain an estimate for ϕ_- we use the Gross equation

$$\begin{aligned}
\phi_-^M(\vec{k}) &= \frac{1}{2\pi^2} \int d^3p [K_{-+}(\vec{k}, \vec{p}) S_+(p) \phi_+^M(\vec{p}) \\
&\quad + K_{--}(\vec{k}, \vec{p}) S_-(p) \phi_-^M(\vec{p})]. \tag{6.4}
\end{aligned}$$

We expect to get a good approximation for ϕ_- by dropping the second term because K_{--} is of second order in k/m , both for PV and for PS coupling, while ϕ_- is of the order of the first term.

Let us now evaluate Eq. (6.2) for the case of PS

$$O_{++}^0(\vec{p}', \vec{p}, \vec{q}) = \frac{1}{8\pi^2 M_N^3} \frac{g^2}{4\pi} F(\vec{k}_r) \vec{q} \cdot \vec{\sigma}^{(1)} \vec{k}_r \cdot \vec{\sigma}^{(2)} \vec{\tau}^{(1)} \cdot \vec{\tau}^{(2)} \left(\frac{F_1^S}{2} + F_2^S \right) + \frac{1}{4\pi^4} \int d^3k K_{-+}(\vec{p}', \vec{k} + \frac{\vec{q}}{2}) \left(-\frac{F_1^S}{M_D} \right) K_{-+}(\vec{k}, \vec{p}). \tag{6.8}$$

The pion momentum is denoted by $\vec{k}_r = \vec{p} + \vec{q}/2 - \vec{p}'$ and the pion propagator and cutoff factors are collected in $F(\vec{k}_r) = (k_r^2 + \mu^2)^{-1} (k_r^2 + \Lambda^2)^{-2} \Lambda^4$. The second term is, in fact, logarithmically divergent, due to the neglect of factors $1/E_k$, without the strong form factors introduced in Eq. (6.5). This term can be written as

$$\frac{1}{16\pi^4 M_N^2 M_D^2} F_1^S \left(\frac{g^2}{4\pi} \right)^2 (\vec{\tau}^{(1)} \cdot \vec{\tau}^{(2)})^2 \int d^3k \left(k^2 - \frac{k_r^2}{4} \right) F\left(\vec{k} - \frac{\vec{k}_r}{2}\right) F\left(\vec{k} + \frac{\vec{k}_r}{2}\right), \tag{6.9}$$

which shows that it is a function of \vec{k}_r only. The easiest way to evaluate this contribution to the charge operator is to make a Fourier transform to configuration space. This "box" terms gives a nonzero contribution at zero momentum transfer because it measures the probability of the deuteron to be in a $^1P_1^-$ or in a $^3P_1^-$ state, and thus we have to renormalize the total wave function. In Fig. 11 we show the absolute values of the contributions from the two terms in Eq. (6.8) to the charge form factor separately. Since they are of opposite sign there are significant cancellations, resulting in a positive net result.

One might wonder whether the negative-energy components of the wave function are well approximated by the iteration with the one-pion-exchange (OPE) kernel. Since, for PS coupling, the OPE kernel is of order k/m and the effective coupling in an isospin zero state is about 42, and all other bosons have a smaller coupling, a larger mass and, most important, are of higher order in k/m , we expect this to be a good approximation. This is demonstrated in Fig. 12 for a model in which we fitted the 3S_1 - 3D_1 channel as well as possible.

coupling. The lowest order approximation to K_{-+} is

$$\begin{aligned}
K_{-+}(\vec{k}, \vec{p}) &= \frac{1}{2M_N} \frac{g^2}{4\pi} \frac{\mathbf{1}^{(1)}(\vec{p} - \vec{k}) \cdot \vec{\sigma}^{(2)}}{(\vec{p} - \vec{k})^2 + \mu^2} \\
&\quad \times \left[\frac{\Lambda^2}{(\vec{p} - \vec{k})^2 + \Lambda^2} \right]^2 \vec{\tau}^{(1)} \cdot \vec{\tau}^{(2)}, \tag{6.5}
\end{aligned}$$

$$K_{+-}(\vec{k}, \vec{p}) = K_{-+}(\vec{p}, \vec{k}). \tag{6.6}$$

Counting powers of k/m in Eq. (6.2) we find that the term proportional to Γ_{--} is not *a priori* small as compared to the other two terms due to the fact that $\tilde{\Gamma}_{--}^0$ is essentially the unit operator. Inserting Eq. (6.4) into Eq. (6.2) and using Eq. (6.5) we find

$$\begin{aligned}
\Delta \langle J_D^{\mu} \rangle_{\text{neg}} &= \int d^3p' d^3p \phi_+^{M\prime\dagger}(\vec{p}') S_+(p') \\
&\quad \times O_{++}^{\mu}(\vec{p}', \vec{p}, \vec{q}) S_+(p) \phi_-^M(\vec{p}), \tag{6.7}
\end{aligned}$$

where the effective two-body operator O is given by

We took the OBE kernel as for PV coupling and found a reasonable fit, with the δ_{3S_1} overall too low by about 8%, for $g_e^2/4\pi = 23.2$, $g_\omega^2/4\pi = 5$, $g_\rho^T/g_\rho^V = 4.0$, and $\Lambda^2 = 1.2$; the other coupling constants are the same as for the PV model. The negative-energy components obtained from this model are very similar to the approximated ones. They also agree with those obtained from a different model in Ref. 18.

We now turn to the positive-energy state contribution to Eq. (6.1), again restricting ourselves to the charge form factor. The most obvious differences between this expression and the nonrelativistic one consist of the boosted argument in the final state wave function, the boost operator in the photon-nucleon vertex, and the occurrence of a relativistic propagator instead of the Lippmann-Schwinger Green's function. The last two differences do not lead to significant changes in the nonrelativistic result for moderate momentum transfers. The difference between using the full relativistic vertex and the nonrelativistic one is shown in Fig. 11. It is much smaller than the other contributions but, due to cancellations, still

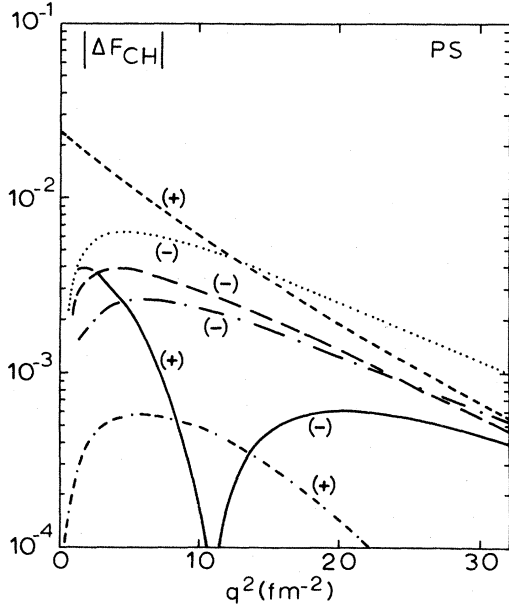


FIG. 11. The absolute values of the corrections to the charge form factor for a PS theory. The sign is given in brackets with each curve. The solid line is the total contribution. The other corrections are the "box" current (---), the terms linear in ϕ_- (- · - ·), the boost effect on the final-state wave function (- · -), and the effect of a relativistic vertex operator (- - -). We also plotted the pair-current contribution (···).

of some significance. The effect of the boosted argument is calculated from the approximated Gross equation

$$\Delta\phi_+^{M\uparrow}(\vec{k}, \frac{\vec{q}}{2}) = \frac{1}{2\pi^2} \int d^3p' \phi_+^{M\uparrow}(\vec{p}') S_+(p') \times \left[K(\vec{p}', \vec{k}') - K(\vec{p}', \vec{k} + \frac{\vec{q}}{2}) \right], \quad (6.10)$$

where we keep only the contribution from the OPE term. Expanding Eq. (6.10) to lowest order in k/m and q/m we find for both PV and PS coupling as the effective two-body operator

$$O_{++}(\vec{p}, \vec{p}', \frac{\vec{q}}{2}) = \frac{1}{8\pi^2 M_N^3} \frac{g^2}{4\pi} F(\vec{k}_\pi) \vec{q} \cdot \vec{\sigma}^{(1)} \vec{k}_\pi \cdot \vec{\sigma}^{(2)} \vec{\tau}^{(1)} \cdot \vec{\tau}^{(2)} \frac{F_1^S}{2}. \quad (6.11)$$

At this point we note that the first term in Eq. (6.8) is not exactly equal to the effective operator corresponding to the so-called pair excitation term, in contrast to what one may naively have expected. The part proportional to F_1^S should be twice as large. Usually the pair term is calculated in the Breit frame, starting from the two diagrams shown in Fig. 13 with the intermediate

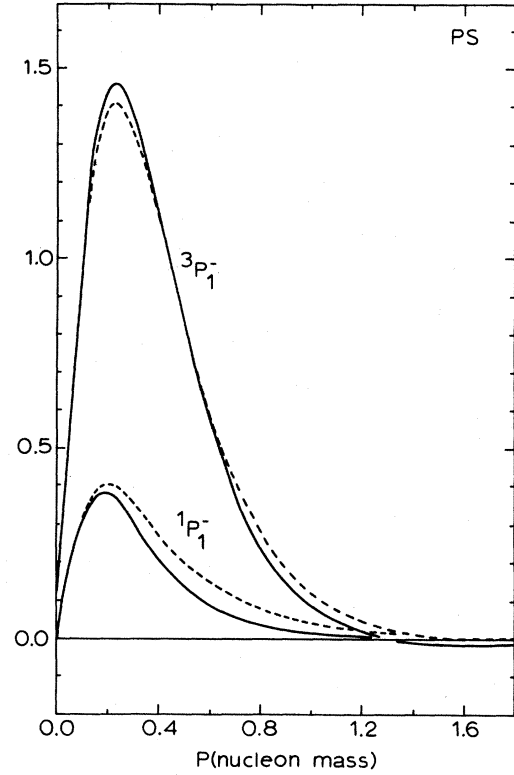


FIG. 12. The negative-energy components of the PS wave function for a model calculation (—) and obtained from iteration of the positive-energy components with the OPE kernel (---).

nucleon being in a negative-energy state. The external particles are taken to be on mass shell and are described by the positive-energy spinors defined in the Appendix. In our formalism the missing term is found as the correction arising from the boosted arguments of the final state and given to lowest order in Eq. (6.11). This is due to the way we evaluate the various contributions. Although we started from the charge operator in the Breit frame, we moved the boost operators, which relate the c.m. frame of the two nucleons to a

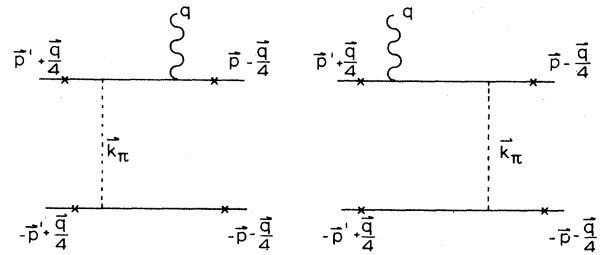


FIG. 13. The diagrams used in perturbative calculations to estimate MEC contributions to the deuteron current. The external particles are on mass shell, indicated by a cross, and the intermediate nucleon can be in a positive- or negative-energy state.

moving frame, to the photon-nucleon vertex. Part of the pair term is now disguised as a boost effect.

Instead of taking the lowest order correction (6.11) we may calculate the difference $\Delta\phi_+$ exactly for the OPE kernel. This leads to small differences between the PV and the PS theory. Furthermore, we used the Reid wave function in Eq. (6.10) to calculate $\Delta\phi_+$. Taking a relativistic wave function instead of the Reid wave function gives virtually the same results for the charge form factor. The contributions to the charge form factor are shown in Fig. 11 for PS coupling and in Fig. 14 for PV coupling.

In the foregoing analysis of the boost effects in the arguments of the wave function we started from the OPE iterated Eq. (6.10). We may also try to estimate this correction by replacing directly the argument of the wave function by the appropriate boosted one, i.e.,

$$\Delta\phi_+^{\dagger}\left(\vec{k}, \frac{\vec{q}}{2}\right) = \phi_{\text{Reid}}^{\dagger}(\vec{k}') - \phi_{\text{Reid}}^{\dagger}\left(\vec{k} + \frac{\vec{q}}{2}\right), \quad (6.12)$$

where \vec{k}' is given by Eq. (5.6). The result is shown in Fig. 14 and is remarkably almost identical to the estimate from the OPE iteration. A closer examination reveals that this can be understood by noting that the largest contributions come from the low momentum parts of the wave function, which are dominated by the OPE.

We now discuss the different effects in a PV coupling theory. We already noted the boost effects on the arguments of the wave function are

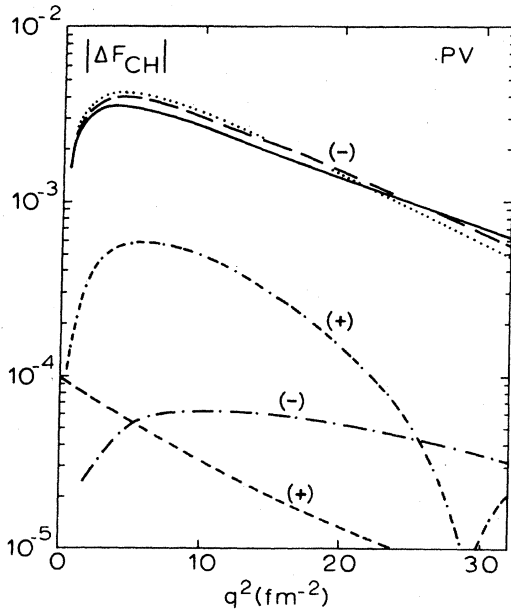


FIG. 14. Same as Fig. 11. The dotted line is the boost effect calculated directly from the Reid wave function, Eq. (6.12).

the same as for the PS coupling theory and qualitatively no differences occur in an exact calculation. The negative-energy-state contributions are shown in Fig. 14. In this case we find much smaller contributions since K_{-+} is now of order $(k/m)^3$ and accordingly the term with Γ_{-+} will be smaller than the terms with Γ_{-} . For the same reason the negative-energy components of the wave function are not approximated very well by the iteration with the OPE model. Figure 9 shows that there are indeed significant contributions from the other bosons.

In Ref. 3 we presented slightly different arguments for the smallness of the exchange-current effects at moderate momentum transfers in the case of PV pion-nucleon interaction. It was found numerically that there is a cancellation between what we called dynamical and exchange effects.¹⁹ This cancellation can be understood in the following way. Consider the OPE diagram for PV coupling. Restricting ourselves to the positive-energy states, and using the Dirac equation, the operator describing this diagram can be written as

$$O^{\text{PV}} = \frac{g^2}{4\pi} \left[\gamma_5^{(1)} \gamma_5^{(2)} - \frac{P_{10} - E_p}{2M_N} \gamma_0^{(1)} \gamma_5^{(1)} \gamma_5^{(2)} + \frac{Q_{10} - E_q}{2M_N} \gamma_0^{(1)} \gamma_5^{(1)} \gamma_5^{(2)} \right] \Delta. \quad (6.13)$$

The momenta are defined in Fig. 15 and a factor $4M_N^2$ has been absorbed into the coupling constant so that it is identical to the one for PS coupling. Furthermore, Δ represents all the factors coming from the cutoff form factor, the pion propagator, and the isopin operators. For on-shell particles, $P_{10} = E_p$ and $Q_{10} = E_q$, only the first term in Eq. (6.13) survives, demonstrating the equivalence between PV and PS coupling for on-mass-shell positive-energy states. When we use the Gross equation we have $P_{10} = 2E - E_p$ and $Q_{10} = 2E - E_q$. As a result the second and the third terms tend to cancel each other. Since the OPE diagram occurs in the relevant diagrams describing the corrections to the nonrelativistic limit of the charge form factor, this cancellation should also take

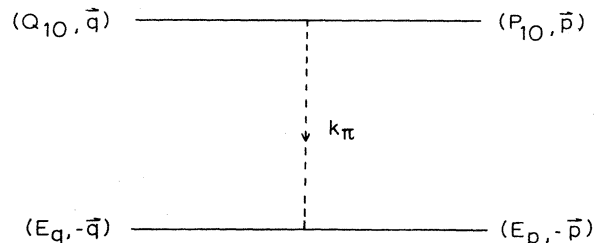


FIG. 15. Definition of the momenta for the OPE diagram; particle 2 is taken to be on the mass shell.

place there. In the usual MEC calculations²⁰ the leading correction is obtained from the diagrams in Fig. 13, with the intermediate nucleon propagating in a positive-energy state. The external nucleons are assumed to be on the mass shell. Furthermore, since the intermediate nucleon is in a positive-energy state the nonrelativistic contribution has to be subtracted. As a result only the second term in Eq. (6.13) is taken into account in the calculation. The correction found in this way is essentially the same as the pair term in a PS theory and is given in Fig. 16. However, the assumption that the external particles can be put on the mass shell in such a MEC treatment can lead to erroneous results. The off-mass-shell correction to the charge form factor, corresponding to the third term in Eq. (6.13), can readily be calculated in the Gross model. The result is also shown in Fig. 16. The contribution is of opposite sign and of the same order of magnitude as the MEC contribution leading to significant cancellations, as expected from our discussion of Eq. (6.13). This shows explicitly that it is not correct to put the external nucleons on the mass shell for PV coupling as is usually done in a MEC calculation.

Two remarks are in order. Firstly, the dynamical correction does not vanish at zero momentum

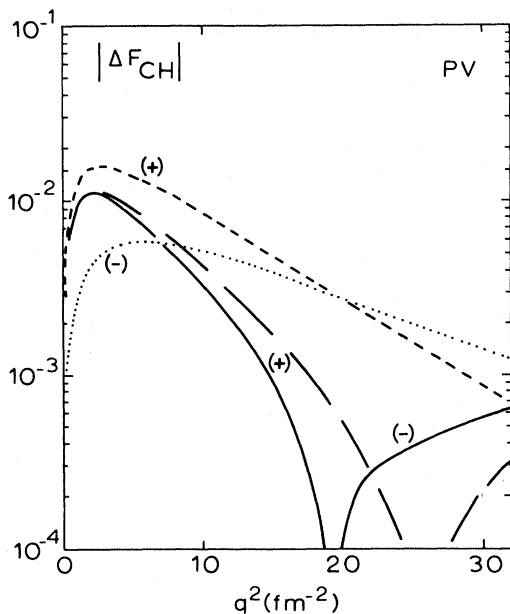


FIG. 16. The various contributions from the positive-energy states, for PV coupling, to the charge form factor: MEC (···); dynamical correction (- - -). The total result is given by (—), and (- - -) is the result when the potential is expanded to lowest order.

transfer. What is shown in Fig. 16 is the difference between the normalized charge form factors,

$$\frac{F_{CH}^{nr}(q^2) + F_{CH}^{dyn}(q^2)}{1 + F_{CH}^{dyn}} - F_{CH}^{nr}(q^2). \quad (6.14)$$

Secondly, in evaluating the contributions of the potential to the diagrams of Fig. 13, we used the relativistic expression for the OPE kernel [the first term in Eq. (6.13)]. Expanding this kernel consistently up to second order in k/m (the first order is zero) and using a static approximation to the pion propagator, we find that the total result does not change qualitatively, as can be seen from Fig. 16.

VII. CONCLUDING REMARKS

Starting from a one-boson-exchange model within a relativistic quasipotential approach, we have shown that in the description of the nucleon-nucleon interaction effects of special relativity such as the presence of negative-energy states can have an important effect on the scattering observables. In general, a reasonable fit is found for the Gross equation except for certain channels such as 3D_1 , 3P_2 , and ϵ_2 , where the phase shift decreases much too fast at higher energies. The negative-energy states in the Gross approximation cause a very large splitting between the 1S_0 and 3S_1 phase shifts. As a result we have to take a rather large value for g_ρ^T/g_ρ^V . Also the strong repulsion in the P waves can only be remedied by a very strong cutoff, which causes the difficulties in the other partial waves. The most important drawback of this equation is, however, that it leads to unphysical singularities, which are present at all energies, if we want to take higher order terms in the kernel into account.

Once a reasonable fit for the scattering parameters is constructed the em properties of the deuteron are found to be very similar to those obtained in a nonrelativistic calculation. We have shown in the previous section that, although separate corrections to the nonrelativistic limit can be considerable, the various terms tend to cancel each other, both in the case of pseudovector and pseudoscalar pion-nucleon coupling. The resulting correction to the charge form factor is small. The cancellation in a pseudoscalar theory is rather remarkable since it does not take place for a given order of the π - N coupling constant. It is, however, not surprising that higher corrections can be important since the coupling between positive- and negative-energy states in such a theory is very strong.

There is another aspect which we have not con-

sidered in Sec. VI and which is much harder to estimate. Namely, the vertex function satisfies some relativistic equation instead of a nonrelativistic Lippman-Schwinger equation. Numerically we find that the differences between a Reid wave function and a solution to the Gross equation, shown in Fig. 8, can be significant for larger values of the relative momentum. As a result the em form factors at high momentum transfer may be sensitive to the specific model chosen. The deviations in the 3D_1 channel are in accord with the lower D -state probability found for the Gross wave functions, and is characteristic for OBE models. However, the charge form factor calculated with the positive-energy components of the PV Gross wave function is quite similar to the result obtained with the Reid wave function. For the PS wave function we find larger deviations, but we have to keep in mind that it is not possible in that case to find a good overall fit to the scattering data. We believe that, once a good fit to the scattering data has been found, the wave functions will produce similar results for the charge form factor.

The fact that we find, in our approach, part of what is conventionally known as the pair excitation current for PS coupling from the boost effects in the arguments of the final state is in accordance with Ref. 21. There it was shown that to lowest order, i. e., linear in ϕ_- , the Gross approximation to the deuteron current gives the same results as the perturbative approach. Our results indicate that the calculation of corrections to a nonrelativistic theory is quite delicate and that it is important to have at least a consistent approach to both the dynamics of the two-nucleon system and the em properties of the deuteron.

Another observation is that, since there are many cancellations, higher order effects may be important so that one is led to consider corrections to the Gross approximation. The results reported here also have some bearing on the calculation of the em properties of more particle systems. One possible way to proceed is along the same lines as we have done in Sec. VI for the deuteron.

This work was supported in part by the Stichting voor Fundamenteel Onderzoek der Materie.

APPENDIX

In this appendix we collect some formulas pertaining to the nonrelativistic reduction of the deuteron current. We introduce spinors that are still operators in spin space, which project on positive and negative energy states:

$$\begin{aligned}\omega_+(\vec{p}) &= \left(\frac{E_p + m}{2E_p}\right)^{1/2} \begin{pmatrix} 1 \\ \frac{\vec{\sigma} \cdot \vec{p}}{E_p + m} \end{pmatrix}, \\ \omega_-(\vec{p}) &= \left(\frac{E_p + m}{2E_p}\right)^{1/2} \begin{pmatrix} \frac{\vec{\sigma} \cdot \vec{p}}{E_p + m} \\ 1 \end{pmatrix}.\end{aligned}\quad (\text{A1})$$

The usual spinors are obtained by operating with ω_{\pm} on the two-component Pauli spinors. The one-particle propagator can be written in terms of ω_{\pm} as

$$(\not{p} - m + i\epsilon)^{-1} = \frac{\omega_+(\vec{p})\bar{\omega}_+(\vec{p})}{p_0 - E_p + i\epsilon} - \frac{\omega_-(-\vec{p})\bar{\omega}_-(-\vec{p})}{p_0 + E_p - i\epsilon}, \quad (\text{A2})$$

which holds in any frame of reference. It is convenient to abbreviate the projection operators in (A2) as

$$\Lambda_{\pm}(\vec{p}) = \omega_{\pm}(\pm\vec{p})\bar{\omega}_{\pm}(\pm\vec{p}). \quad (\text{A3})$$

In the reduction of the Gross equation we encounter the positive- and negative-energy projections of the vertex function

$$\phi_{\pm}^M(\vec{p}) = \bar{\omega}_{\pm}^{(1)}(\pm\vec{p})\bar{\omega}_{\pm}^{(2)}(-\vec{p})\psi_{\text{c.m.}}^M(\vec{p}) \quad (\text{A4})$$

defined in the c.m. frame.

To write the matrix elements of the deuteron current in terms of these projections we have to use the fact that

$$\Lambda_-^{(2)}(-\vec{k}')\gamma_0^{(2)}[\Lambda^{(2)}(\mathcal{L})]^2\Lambda_+^{(2)}(-\vec{k}) = 0, \quad (\text{A5})$$

where k and k' are connected by the Lorentz transformation \mathcal{L} :

$$k' = \mathcal{L}\left(k + \frac{q}{2}\right), \quad k_0 = E - E_k, \quad k'_0 = E - E_{k'}. \quad (\text{A6})$$

Equation (A5) ensures that only positive-energy states propagate for particle two, i. e., when we insert the unit operator for particle 2

$$1^{(2)} = \Lambda_+^{(2)}(-\vec{k}')\gamma_0^{(2)} + \Lambda_-^{(2)}(-\vec{k}')\gamma_0^{(2)} \quad (\text{A7})$$

in the expression for the current we can drop the second term. Defining

$$\tilde{\Gamma}_{\alpha,\beta}^{\mu} = \bar{\omega}_{\alpha}^{(1)}(\alpha\vec{k}')\omega_{\beta}^{(2)\dagger}(-\vec{k}')\tilde{\Gamma}^{\mu}(q)\omega_{\beta}^{(1)}(\beta\vec{k})\omega_{\alpha}^{(2)}(-\vec{k}) \quad (\text{A8})$$

and

$$S_+(k) = \frac{1}{2(E_k - E)}, \quad S_-(k) = -\frac{1}{2E}, \quad (\text{A9})$$

the expression for the matrix elements of J_D^{μ} , Eq. (5.2), can be written as

$$\langle P+q, M' | J_D^\mu | P, M \rangle = \int d^3k \sum_{\alpha, \beta} \phi_\alpha^{M'+}(\vec{k}') S_\alpha(k') \bar{\Gamma}_{\alpha, \beta}^\mu S_\beta(k) \phi_\beta^M(\vec{k}). \quad (\text{A10})$$

The relation between the two-particle spin states

$$|\vec{p}; \lambda_1 \lambda_2 \rho_1 \rho_2 \rangle_{\text{spin}} = \omega_{\rho_1}^{(1)}(\rho_1 \vec{p}) \omega_{\rho_2}^{(2)}(-\rho_2 \vec{p}) \otimes \chi_{\rho_1 \lambda_1}^{(1)} \chi_{\rho_2 \lambda_2}^{(2)} \quad (\text{A11})$$

and the helicity states introduced in Ref. 1 is

$$\begin{aligned} \langle \vec{p}; \lambda_1' \lambda_2' \rho_1' \rho_2' | \vec{p}; \lambda_1 \lambda_2 \rho_1 \rho_2 \rangle_{\text{helicity}} \\ = \delta_{\rho_1' \rho_1} \delta_{\rho_2' \rho_2} D_{\lambda_1' \lambda_1}^{1/2}(\phi_p, \theta_p, -\phi_p) * D_{\lambda_2' -\lambda_2}^{1/2} \\ \times (\phi_p, \theta_p, -\phi_p). \end{aligned} \quad (\text{A12})$$

With this transformation matrix, and the decomposition of the unit operator

$$1 = \sum_{\lambda_1 \rho_1} \sum_{\lambda_2 \rho_2} (-1)^{\rho_1 - \rho_2} |\vec{p}; \lambda_1 \lambda_2 \rho_1 \rho_2 \rangle_{\text{spin}} \langle \vec{p}; \lambda_1 \lambda_2 \rho_1 \rho_2 |, \quad (\text{A13})$$

the partial wave expansion of the vertex function is

found to be very similar to the nonrelativistic case,

$$\psi^M(\vec{p}) = \sum_{L, S, \rho} Y_{M\rho}^{JLS}(\vec{p}) \phi_{LS}^\rho(p), \quad (\text{A14})$$

where

$$Y_{M\rho}^{JLS}(\vec{p}) = \sum_{m, \mu} C_{m\mu M}^{LSJ} Y_L^m(\Omega_{\vec{p}}) \chi_{\mu, \rho}^S(\vec{p}) \quad (\text{A15})$$

and

$$\chi_{\mu, \rho}^S(\vec{p}) = (-1)^{\rho_1 - \rho_2} \sum_{\lambda_1, \lambda_2} C_{\lambda_1 \lambda_2 \mu}^{1/2 1/2 S} |\vec{p}; \lambda_1 \lambda_2 \rho_1 \rho_2 \rangle_{\text{spin}}. \quad (\text{A16})$$

In the nonrelativistic limit only the positive-energy states survive and they reduce to the usual states

$$\lim_{nr} \chi_{\mu, \rho}^S(\vec{p}) = \sum_{\lambda_1 \lambda_2} C_{\lambda_1 \lambda_2 \mu}^{1/2 1/2 S} \chi_{\lambda_1}^{(1)} \chi_{\lambda_2}^{(2)}. \quad (\text{A17})$$

For this reason, and because of the compact notation (A1), it is natural to use these states instead of helicity states when discussing the nonrelativistic limit.

¹M. J. Zuilhof and J. A. Tjon, Phys. Rev. C 22, 2369 (1980).

²F. Gross, Phys. Rev. 186, 1448 (1969).

³J. A. Tjon and M. J. Zuilhof, Phys. Lett. 84B, 31 (1979).

⁴G. E. Brown and A. D. Jackson, *The Nucleon-Nucleon Interaction* (North-Holland, Amsterdam, 1976).

⁵R. Yaes, Phys. Rev. D 3, 3086 (1971).

⁶R. Blankenbecker and R. Sugar, Phys. Rev. 142, 1051 (1966).

⁷J. J. Kubis, Phys. Rev. D 6, 547 (1972).

⁸H. P. Noyes, Phys. Rev. Lett. 15, 538 (1965); K. L. Kowalski, *ibid.* 15, 798 (1965).

⁹M. H. MacGregor, R. A. Arndt, and R. M. Wright, Phys. Rev. 182, 1714 (1969).

¹⁰R. A. Arndt private communication from R. A. Bryan.

¹¹L. Müller and W. Glöckle, Nucl. Phys. B146, 393 (1978).

¹²G. Passarino and M. Veltman, Nucl. Phys. B160, 151

(1979).

¹³M. Veltman (unpublished).

¹⁴H. Strubbe, Comput. Phys. Commun. 8, 1 (1974); 18, 1 (1979).

¹⁵A. D. Jackson, A. Landé, and D. O. Riska, Phys. Lett. 55B, 23 (1975).

¹⁶M. Garí and H. Hyuga, Nucl. Phys. A264, 409 (1975).

¹⁷R. G. Arnold, C. E. Carlson, and F. Gross, Phys. Rev. C 21, 1426 (1980).

¹⁸W. W. Buck and F. Gross, Phys. Rev. D 20, 2361 (1979).

¹⁹The various corrections shown in Fig. 2 of Ref. 3 are too large by a factor of 2 due to an error in counting diagrams that contribute.

²⁰D. Drechsel and H. J. Weber, Nucl. Phys. A256, 317 (1976).

²¹F. Gross, in *Few-body Systems and Nuclear Forces I*, Lecture notes in Physics, edited by H. Zingl *et al.* (Springer, Berlin, 1978), Vol. 82.